

New Star-Shaped Luminescent Triarylamines: Synthesis, Thermal, Photophysical, and Electroluminescent Characteristics

K. R. Justin Thomas,[†] Jiann T. Lin,^{*,†,‡} Yu-Tai Tao,^{*,†} and Chung-Wen Ko[†]

*Institute of Chemistry, Academia Sinica, Taipei, Taiwan 115, Republic of China, and
Department of Chemistry, National Central University, Chungli,
Taiwan 320, Republic of China*

Received October 10, 2001. Revised Manuscript Received January 3, 2002

A series of 3,6-disubstituted carbazole and 1,3,5-trisubstituted benzene derivatives incorporating thienyl aromatic (phenyl, fluorenyl, and carbazoyl) conjugation and end-capped diphenylamine were synthesized by iterative C–N and C–C coupling procedures. The carbazole derivatives emit blue light and the star-shaped benzene derivatives emit either blue or bluish green color depending on the conjugation segment. In general, they possess high glass transition temperatures (>120 °C) and decomposition temperatures (>520 °C). Double-layer organic light-emitting devices were successfully fabricated using these novel molecules as hole-transporting and emitting materials. Devices of the configuration ITO/HTM/TPBI/Mg:Ag display blue to green emission from the HTM layer while in the devices of the configuration ITO/HTM/Alq₃/Mg:Ag, a typical green emission from the Alq₃ layer was observed.

Introduction

Organic light-emitting diodes (OLED) based on thin layers of small molecules^{1–3} and polymers^{4–6} continue

to attract wide attention owing to the numerous application possibilities including flat-panel displays. Design and synthesis of hole-transporting materials,^{7–9} a compelling constituent in OLED, have significantly advanced since the multilayered OLEDs were demonstrated by Tang and VanSlyke.¹⁰ Triarylamines (simple, branched, and star-shaped) were reported to effectively act as hole-transporting materials.^{7,11} However, because of the inherent reductive quenching, most triarylamines are either nonluminescent or only weakly emitting. Additionally, larger star-shaped triarylamines easily form exciplexes when contacted with the electron-transporting or emitting layers.¹² Exciplex formation normally affects the efficiency of a multilayer device. Efforts directed toward preventing such formation are scarce and few technical alternatives have been exemplified.¹³

We have initiated a program to explore star-shaped triarylamines with featured chromophores. Pyrene-

* To whom correspondence should be addressed. Fax: Int. code +(2)27831237. E-mail: jtlin@chem.sinica.edu.tw.

[†] Academia Sinica.

[‡] National Central University.

(1) (a) Segura, J. L. *Acta Polym.* **1998**, *49*, 319. (b) Shirota, Y. *J. Mater. Chem.* **2000**, *1*.

(2) (a) Noda, T.; Shirota, Y. *J. Am. Chem. Soc.* **1998**, *120*, 9714. (b) Lu, P.; Hong, H.; Cai, G.; Djurovich, P.; Weber, W. P.; Thompson, M. E. *J. Am. Chem. Soc.* **2000**, *122*, 7480. (c) Shirota, Y.; Kinoshita, M.; Noda, T.; Okumoto, K.; Ohara, T. *J. Am. Chem. Soc.* **2000**, *122*, 11021. (d) Freeman, A. W.; Koene, S. C.; Malenfant, P. R. L.; Thompson, M. E.; Fréchet, J. M. J. *J. Am. Chem. Soc.* **2000**, *122*, 12385. (e) Wang, C.; Jung, G.-Y.; Hua, Y.; Pearson, C.; Bryce, M. R.; Petty, M. C.; Batsanov, A. S.; Goeta, A. E.; Howard, J. A. K. *Chem. Mater.* **2001**, *13*, 1167. (f) Tao, Y.-T.; Balasubramian, E.; Danel, A.; Jarosz, B.; Tomasik, P. *Chem. Mater.* **2001**, *13*, 1207.

(3) (a) Yu, G.; Liu, Y.; Wu, X.; Zhu, D.; Li, H.; Jin, L.; Wang, M. *Chem. Mater.* **2000**, *12*, 2537. (b) Schmitz, C.; Schmidt, H.-W.; Thelakkat, M. *Chem. Mater.* **2000**, *12*, 3012. (c) Leung, L. M.; Lo, W. Y.; So, S. K.; Lee, K. M.; Choi, W. K. *J. Am. Chem. Soc.* **2000**, *122*, 5640. (d) Gao, F. G.; Bard, A. J. *J. Am. Chem. Soc.* **2000**, *122*, 7426. (e) Lamansky, S.; Djurovich, P.; Murphy, D.; Abdel-Razzaq, F.; Lee, H.-E.; Adachi, C.; Burrows, P. E.; Forrest, S. R.; Thompson, M. E. *J. Am. Chem. Soc.* **2001**, *123*, 4304.

(4) (a) Kraft, A.; Grimsdale, A. C.; Holmes, A. B. *Angew. Chem., Int. Ed.* **1998**, *37*, 402. (b) Mitschke, U.; Bäuerle, P. *J. Mater. Chem.* **2000**, *10*, 1471.

(5) (a) Burroughs, J. H.; Bradley, D. D. C.; Brown, A. R.; Marks, R. N.; Mackay, K.; Friend, R. H.; Burn, P. L.; Holmes, A. R. *Nature* **1990**, *347*, 539. (b) Cao, Y.; Parker, I. D.; Yu, G.; Zhang, C.; Heeger, A. J. *Nature* **1999**, *374*, 414. (c) Miteva, T.; Meisel, A.; Knoll, W.; Nothofer, H. G.; Scherf, U.; Müller, D. C.; Meerholz, K.; Yasuda, A.; Neher, D. *Adv. Mater.* **2001**, *13*, 565. (d) Wang, C.; Kilitziraki, M.; Pålsson, L.-O.; Bryce, M. R.; Monkman, A. P.; Samuel, I. D. W. *Adv. Funct. Mater.* **2001**, *11*, 47.

(6) (a) Pei, J.; Yu, W.-L.; Huang, W.; Heeger, A. J. *Macromolecules* **2000**, *13*, 2462. (b) Liu, S.; Jiang, X.; Ma, H.; Liu, M. S.; Jen, A. K.-Y. *Macromolecules* **2000**, *33*, 3514. (c) Santerre, F.; Bedja, I.; Dodelet, J. P.; Sun, Y.; Lu, J.; Hay, A. S.; D'Iorio, M. *Chem. Mater.* **2001**, *13*, 1739. (d) Bouillud, A. D.; Lévesque, I.; Toa, Y.; D'Iorio, M.; Beaupré, S.; Blondin, P.; Ranger, M.; Bouchard, J.; Leclerc, M. *Chem. Mater.* **2000**, *12*, 1931.

(7) (a) Forrest, S. R.; Burrows, P. E.; Thompson, M. E. *Chem. Ind.* **1998**, 1022. (b) Chang, S. C.; Liu, J.; Bharathan, J.; Yang, Y.; Onohara, J.; Kido, J. *Adv. Mater.* **1999**, *11*, 734.

(8) (a) Katsumo, K.; Shirota, Y. *Adv. Mater.* **1998**, *10*, 223. (b) O'Brien, D. F.; Burrows, P. E.; Forrest, S. R.; Koene, B. E.; Loy, D. E.; Thompson, M. E. *Adv. Mater.* **1998**, *10*, 1108.

(9) Okumoto, H.; Yatabe, T.; Shimomura, M.; Kaito, A.; Minami, N.; Tanabe, Y. *Adv. Mater.* **2001**, *13*, 72.

(10) Tang, C. W.; VanSlyke, S. A. *Appl. Phys. Lett.* **1987**, *51*, 913.

(11) (a) Ueta, E.; Nakano, H.; Shirota, Y. *Chem. Lett.* **1994**, *12*, 2397.

(b) Noda, T.; Imae, I.; Noma, N.; Shirota, Y. *Adv. Mater.* **1997**, *9*, 239.

(c) Jonda, C.; Mayer, A. B. R.; Thelakkat, M.; Schmidt, H.-W.; Schreiber, A.; Haarer, D.; Terrell, D. *Adv. Mater. Opt. Electron.* **1999**, *9*, 117. (d) Bach, U.; De Cloedt, K.; Spreitzer, H.; Grätzel, M. *Adv. Mater.* **2000**, *12*, 1060.

(12) (a) Tamoto, N.; Adachi, C.; Nagai, K. *Chem. Mater.* **1997**, *9*, 1077. (b) Itano, K.; Ogawa, H.; Shirota, Y. *Appl. Phys. Lett.* **1998**, *72*, 636. (c) Antoniadis, H.; Inbasekaran, M.; Woo, E. *Appl. Phys. Lett.* **1998**, *73*, 3055.

(13) For instance, insertion of a thin buffer layer between HTL and ETL suppresses exciplex formation.

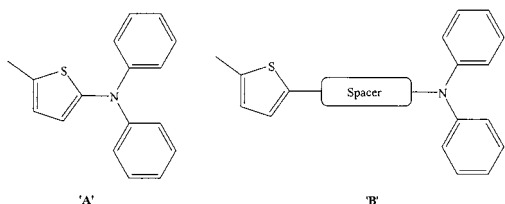


Figure 1. Structure of the building blocks.

incorporated 3,6-carbazole diamines were found to be potential green emitters.¹⁴ Similarly, hexathienylbenzene-based, star-shaped hexamines served as promising hole-transporting materials.¹⁵ However, the latter molecules were largely nonluminescent. It was felt that the close association of the thiophene with the diarylamine unit ("A" in Figure 1) significantly contributed to the emission quenching.¹⁶ It is our idea that the insertion of phenyl or polyaromatics such as fluorene and carbazole between thiophene and the diarylamine unit might improve the emission characteristics.¹⁷ Toward this end we have designed a series of new building blocks of the type "B" (Figure 1), thiophene-Ar-NPh₂ and used them to assemble star-shaped amines utilizing 3,6-disubstituted carbazole and 1,3,5-trisubstituted benzene as the central units. Use of sterically more demanding spacers is also expected to inhibit intermolecular interactions that could give rise to exciplex emission.

In this paper, we present a systematic study on the thermal and the photophysical properties of the star-shaped amines (Chart 1). In an effort to utilize these molecules in OLEDs we have fabricated two-layer devices using these amines as hole-transporting layers. For each amine, two devices were made by changing the electron-transporting layer from Alq₃ (tris(8-hydroxyquinoline)aluminum to TPBI (1,3,5-tris(*N*-phenylbenzimidazol-2-yl)benzene). The energy barriers between the charge transport layers play an important role in shifting the recombination zone from HTL to ETL and influences the performance of the devices.

Experimental Section

General Information. Unless otherwise specified, all the reactions were performed under a nitrogen atmosphere using standard Schlenk techniques. Toluene was distilled from sodium and benzophenone under a nitrogen atmosphere. Dichloromethane and dimethylformamide were distilled from calcium hydride under a nitrogen atmosphere. ¹H and ¹³C NMR spectra were recorded on a Bruker 300-MHz spectrometer operating at 300.135 and 75.469 MHz, respectively. Emission spectra were recorded on a Perkin-Elmer spectrofluorometer. All chromatographic separations were carried out on silica gel (60 M, 230–400 mesh). DSC measurements were carried out on a Perkin-Elmer differential scanning calorimeter at a heating rate of 10 °C/min under a nitrogen atmosphere. TGA measurements were performed on a TA-7 series thermo-

gravimetric analyzer at a heating rate of 10 °C/min under a flow of air. Diphenylamine, Pd(dba)₂, and 1,3,5-tribromobenzene were procured from commercial sources and used as received. 3,6-Dibromo-9-phenylcarbazole,¹⁸ 3,6-dibromo-9-ethylcarbazole,¹⁹ 3-bromo-9-ethylcarbazole,²⁰ 2,7-dibromo-9,9-diethylfluorene,²¹ **1a**, and **2a** were synthesized by following the literature procedures.²² Preparation and characterization of the thiophene incorporated amines (**1b–1e**) and their stannylene derivatives (**2b–2e**) are provided in the Supporting Information. Compounds **3a–e** were synthesized by similar procedures, and only the preparation of **3a** will be described in detail. Compounds **4a–e** were also synthesized by similar procedures, and only the preparation of **4a** will be described. Others are deposited as Supporting Information.

9-Phenyl-3,6-bis{5-[4-diphenylaminophenyl]thiophen-2-yl}-9H-carbazole (3a). A Schlenk tube was charged with 3,6-dibromo-*N*-phenylcarbazole (401 mg, 1 mmol), 4-(5-tributylstannyl-2-thienyl)triphenylamine (**2a**) (1.36 g, 2.2 mmol), Pd(PPh₃)₂Cl₂ (14 mg, 0.002 mmol), and 10 mL of dimethyl formamide and heated at 60–70 °C for 18 h. The reaction was quenched by the addition of methanol and the yellow precipitate formed was collected by filtration. It was dissolved in dichloromethane and purified by column chromatography on silica gel. The second yellow band contained the title compound in 76% (680 mg) yield. ¹H NMR (CDCl₃, δ): 7.00–7.14 (m, 18 H), 7.25–7.30 (m, 9 H), 7.37 (d, *J* = 8.5 Hz, 2 H), 7.44–7.54 (m, 6 H), 7.56–7.69 (m, 6 H), 8.38 (d, *J* = 1.2 Hz, 2 H). ¹³C NMR (CDCl₃, δ): 110.3, 117.5, 123.0, 123.2, 123.8, 124.5, 126.3, 127.0, 127.7, 129.3, 130.0, 140.8, and 147.1. FAB mass (*m/z*): 893 (M⁺). Anal. Calcd for C₆₂H₄₃N₃S₂: C, 83.28; H, 4.85; N, 4.70. Found: C, 83.02; H, 4.84; N, 4.62.

1,3,5-Tris{5-(4-diphenylaminophenyl)thiophen-2-yl}benzene (4a). **4a** was prepared from **2a** and 1,3,5-tribromobenzene in 77% yield as described for **3a**. ¹H NMR (CDCl₃, δ): 7.01–7.06 (m, 12 H, NPh₂ and Ph), 7.08–7.14 (m, 12 H, NPh₂), 7.21 (d, *J* = 3.7 Hz, 3 H, thiophene), 7.24–7.29 (t, *J* = 7.9 Hz, 12 H, NPh₂), 7.35 (d, *J* = 3.7 Hz, 3 H, thiophene), 7.47–7.52 (m, 6 H, Ph), 7.70 (s, 3 H, central Ph ring). ¹³C NMR (CDCl₃, δ): 121.5, 123.1, 123.6, 124.6, 124.7, 126.5, 128.2, 129.3, 135.46, 141.7, 144.1, and 147.4. FAB mass (*m/z*): 1053 (M⁺). Anal. Calcd for C₇₂H₅₁N₃S₃: C, 82.02; H, 4.88; N, 3.99. Found: C, 81.58; H, 4.91; N, 3.76.

LEDs Fabrication and Measurement. Electron-transporting materials TPBI (1,3,5-tris(*N*-phenylbenzimidazol-2-yl)benzene) and Alq₃ (tris(8-hydroxyquinoline) aluminum) were synthesized according to literature procedures^{23,24} and were sublimed twice prior to use. Prepatterned ITO substrates with an effective individual device area of 3.14 mm² were cleaned as described in a previous report.¹⁴ Double-layer EL devices using the compound **3** or **4** as the hole-transport layer and TPBI or Alq₃ as the electron-transport layer were fabricated. For comparison, a typical device using NPD (1,4-bis(1-naphthylphenyl)aminobiphenyl) as the hole-transport layer was also prepared. All devices were prepared by vacuum deposition of 400 Å of the hole-transporting layer, followed by 400 Å of TPBI or Alq. An alloy of magnesium and silver (≈10:1, 500 Å) was deposited as the cathode, which was capped with 1000 Å of silver. The *I–V* curve was measured on a Keithley 2400 Source Meter in an ambient environment. Light intensity was measured with a Newport 1835 Optical Meter.

(14) (a) Justin Thomas, K. R.; Lin, J. T.; Tao, Y.-T.; Ko, C.-W. *Adv. Mater.* **2000**, *12*, 1949. (b) Justin Thomas, K. R.; Lin, J. T.; Tao, Y.-T.; Ko, C.-W. *J. Am. Chem. Soc.* **2001**, *123*, 9404.

(15) Wu, I.-Y.; Lin, J. T.; Tao, Y.-T.; Balasubramaniam, E. *Adv. Mater.* **2000**, *12*, 668.

(16) (a) Tour, J. M. *Chem. Rev.* **1996**, *96*, 537. (b) Sokolowski, M.; Bauerle, P. *Chem. Eur. J.* **1998**, *4*, 2211. (c) Mitschke, U.; Osteritz, E. M.; Debaerdemaeker, T.; Huang, W.; Meng, H.; Yu, W. L.; Pei, J.; Chen, Z. K.; Lai, Y. H. *Macromolecules* **1999**, *32*, 118. (d) Mitschke, U.; Debaerdemaeker, T.; Bauerle, P. *Eur. J. Org. Chem.* **2000**, 425.

(17) (a) Noda, T.; Ogawa, H.; Noma, N.; Shirota, Y. *Appl. Phys. Lett.* **1997**, *70*, 699. (b) Hiromitsu-Ogawa, T.; Noma, N.; Shirota, Y. *J. Mater. Chem.* **1999**, 2177.

(18) Park, M.; Buck, J. R.; Rizzo, C. J. *Tetrahedron* **1998**, *54*, 12707.

(19) Smith, K.; James, D. M.; Mistry, A. G.; Bye, M. R.; Faulkner, D. J. *Tetrahedron* **1992**, *48*, 7479.

(20) Steinhoff, H. *J. Org. Chem.* **1964**, *29*, 2808.

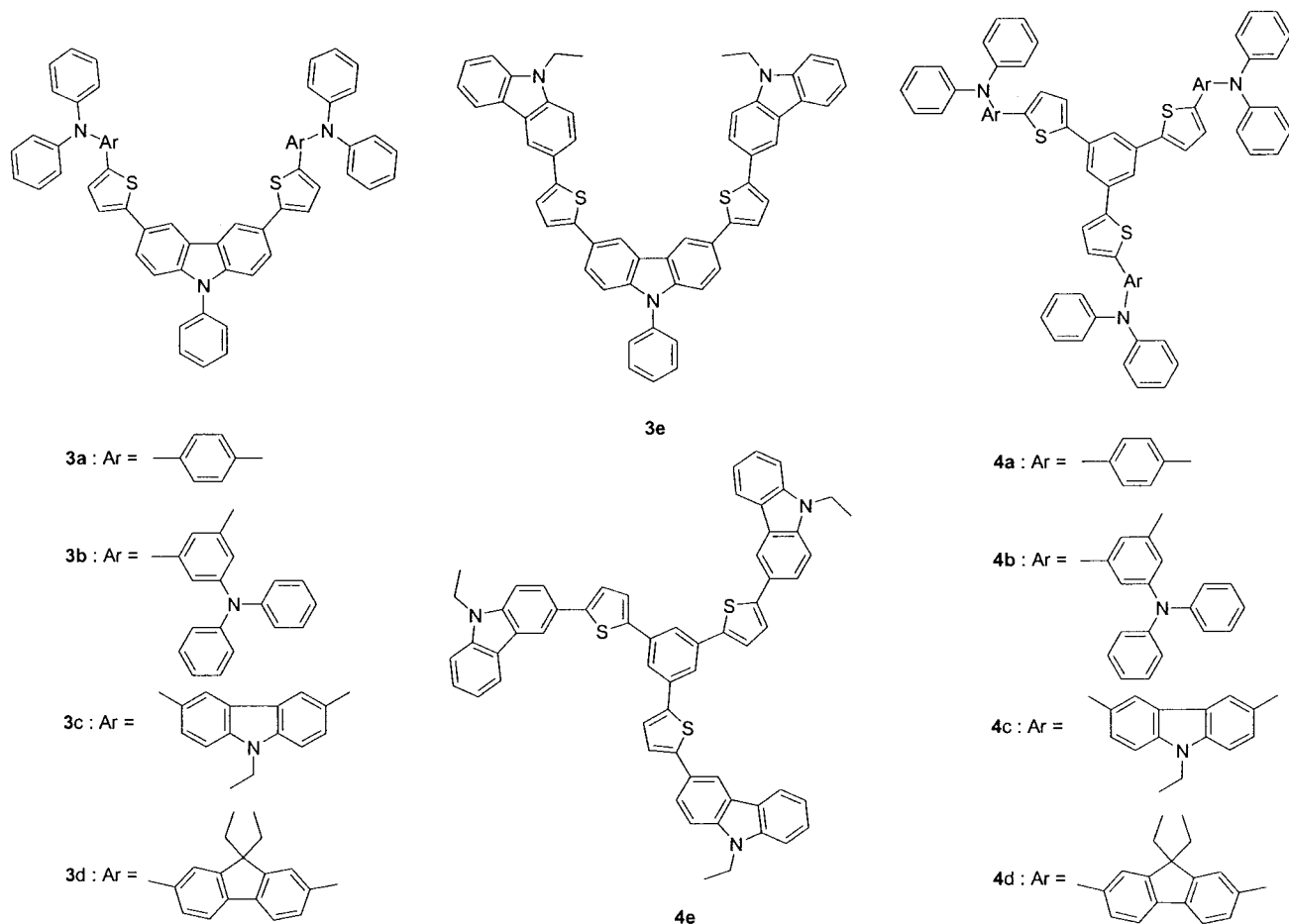
(21) Tsuie, B.; Reddinger, J. L.; Sotzing, G. A.; Soloduchko, J.; Katritzky, A. R.; Reynolds, J. R. *J. Mater. Chem.* **1999**, *9*, 2189.

(22) Wu, X.; Wu, J.; Liu, Y.; Jen, A. K.-Y. *J. Am. Chem. Soc.* **1999**, *121*, 472.

(23) Chen, C. H.; Shi, J.; Tang, C. W. *Coord. Chem. Rev.* **1998**, *171*, 161.

(24) (a) Sonsale, A. Y.; Gopinathan, S.; Gopinathan, C. *Indian J. Chem.* **1976**, *14*, 408. (b) Shi, J.; Tang, C. W.; Chen, C. H. U.S. Patent 5,645,948, 1997.

Chart 1

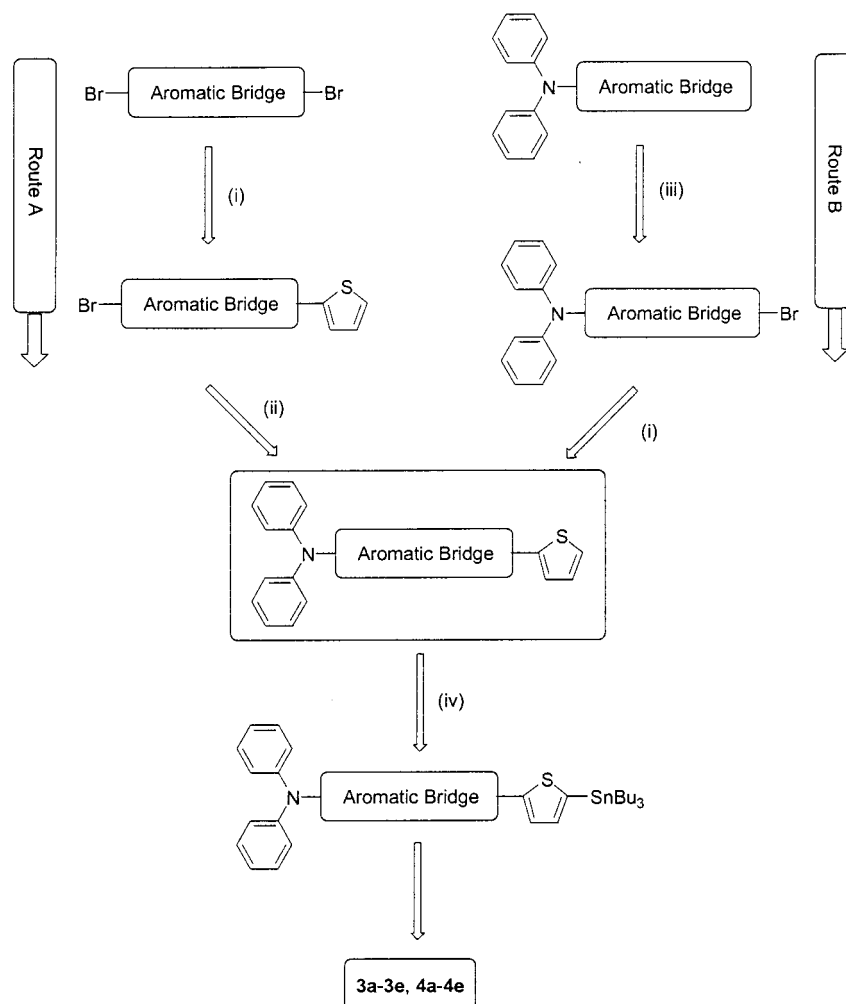


Results and Discussion

Synthesis of the Materials and Thermal Properties. The thiophene-substituted triarylamines required for the present study were made available by two different routes (Scheme 1). In route A, an aromatic dihalide was monotheniylated by Stille coupling with thienyl tri-*n*-butyl stannane, and subsequent C–N coupling reaction with diphenylamine yielded the desired precursors. Alternatively (route B) the triarylamine was first monobrominated by NBS/DMF and subsequent palladium(0)-catalyzed cross-coupling of the bromo derivative with thienyl tri-*n*-butyl stannane leads to the formation of the thienyl-triarylamine congeners. These thiophene derivatives were conveniently converted into the required stannanes by the routine procedures involving lithiation followed by quenching with tri-*n*-butyl tin chloride.^{15,22} 2- or 3-fold palladium-catalyzed Stille coupling of these stannanes with 3,6-dibromo-9-ethylcarbazole or 1,3,5-tribromobenzene provided the target molecules **3a–3e** or **4a–4e** in good yields.

All these materials are soluble in common organic solvents and appear yellow in color. They were characterized by ¹H and ¹³C NMR, mass spectra and elemental analyses. The data are consistent with the proposed structural formulations (Chart 1). Amorphous glass-forming propensity and thermal stability of the compounds were examined by DSC and TGA methods (Table 1). All the compounds easily form stable glasses. The glass transition temperature (*T*_g) was estimated

from DSC curves. The *T*_g of the compounds are higher than the commonly used hole-transporting materials NPB and TPD.^{1b} In general, for the same structural motif the carbazole-based bi-armed materials possess a slightly higher glass transition temperature than the one derived from tri-armed benzene. Replacement of the phenyl group separating the thiophene and the diphenylamine unit by a fluorene or carbazole unit raises the *T*_g significantly. Among these spacers carbazolyl moiety is particularly beneficial for raising glass transition temperature. For the spacers the *T*_g is ordered as carbazole > fluorene > phenyl. The carbazole-containing compounds possess significantly higher *T*_g when compared to the fluorene analogues (**3c** vs **3d** and **4c** vs **4d**). Such an outcome may be due to the presence of two flexible ethyl substituents in the latter as well as the less polar character of the fluorene moiety. This is consistent with our previous observation.^{14b} The decomposition temperature (*T*_d) of the molecules in this study were also affected by the spacers. However, the order of *T*_d among the spacers is rather different: phenyl > carbazole > fluorene. Presumably, the initial loss of ethyl substituents on carbazole and fluorene explains the relatively easy decomposition of **3c** and **3d** (or **4c** and **4d**). In general, the thermal stability of the benzene derivatives (**4a–4d**) surpasses that of the carbazole derivatives (**3a–3d**) because of the larger number of aromatic rings in the former. However, the removal of diphenylamino cap reverses the thermal trends realized so far. Thus, the carbazole derivative **3e** is more stable

Scheme 1. General Synthetic Scheme^a

^a (i) Pd(PPh₃)₂Cl₂, DMF, 2-(tributylstannyl)thiophene; (iii) Ph₂NH, Pd(dba)₂, *t*-BuONa, toluene; (iii) NBS, DMF; (iv) *n*-BuLi, Bu₃SnCl.

Table 1. Physical Data for the Compounds

compd	T_g^a (°C)	T_d^b (°C)	λ_{\max} ($\epsilon_{\max} \times 10^{-3}$) ^c (nm)	λ_{em} (ϕ_f) ^d (nm)	λ_{em}^e (nm)	E_{ox} (ΔE_p) ^f (mV)	HOMO/LUMO ^g (eV)
3a	128	545	376(75.1), 308(38.9)	462, 441 (0.51)	486	313 (95), 562 (64), 823 (62)	5.113/2.293
3b	146	560	321 (237.2)	427, 441 (0.21)	473, 494	+462 (135)	5.262/2.308
3c	178	534	355(85.3), 313(79.1)	451, 431 (0.26)	506	205 (83), 489 (86)	5.008/2.122
3d	156	524	394 (106.6), 315 (39.05)	450, 473 (0.31)	496	+321 (79), 472 (71), 671 (60)	5.121/2.364
3e	142	580	348 (119.6)	421, 445 (0.27)	513	+203 (124)	5.003/2.083
4a	125	596	388(109.0), 304(59.9)	465 (0.36)	495	+419 (112)	5.219/2.431
4b	142	600	307 (285.0)	468 (0.09)	464	+492 (112)	5.292/2.190
4c	176	575	369(84.1), 311(87.0)	501 (0.18)	498	+218 (88), +701 (59)	5.018/2.132
4d	150	562	398 (168.0), 313 (66.13)	488 (0.36)	492	+353 (93), 764 (60), 869 (80)	5.153/2.426
4e	143	565	364 (201.1)	437 (0.42)	492	+341 (133)	5.141/2.187
NPB	103	na	342, 271	450	445	+340 (66)	5.23/2.20
ITO							4.70 (E_F)/na
TPBI	na	na	304	376	375	+1300 (i)	6.20/2.70
Alq ₃	177	428	385	510 (0.15)	534	na	6.09/2.95
Mg:Ag							na/3.70 (E_F)

^a Obtained from DSC measurements. ^b Obtained from TGA measurements. ^c Measured in a CH₂Cl₂ solution, ϵ_{\max} in M⁻¹cm⁻¹ in parentheses. ^d Measured in a CH₂Cl₂ solution; ϕ_f fluorescence quantum yield. ^e Film samples. ^f Measured in CH₂Cl₂. All E_{ox} data are reported relative to ferrocene, which has an E_{ox} at 223 mV relative to Ag/Ag⁺ and the anodic peak–cathodic peak separation (ΔE_p) is 75 mV. The concentration of the compounds used in this experiment was 2.5×10^{-4} M and the scan rate was 100 mV s⁻¹. ^g na, not available.

than the benzene star **4e**. The difference may be due to the presence of three *N*-ethyl carbazole moieties in **4e**, while there are two *N*-ethyl carbazole and one *N*-phenyl carbazole moieties in **3e**. We previously found that the *N*-phenyl carbazole unit was much better than the *N*-ethyl carbazole unit in enhancing the thermal stability of compounds.^{14b}

Optical Properties. The photophysical properties of the molecules were examined by UV–vis and fluorescence spectroscopy in dichloromethane solution. The lowest energy absorption of the compounds is located in the range 307–398 nm. In general, the benzene derivatives, except **4b**, exhibit bathochromically shifted absorptions with larger extinction coefficients as com-

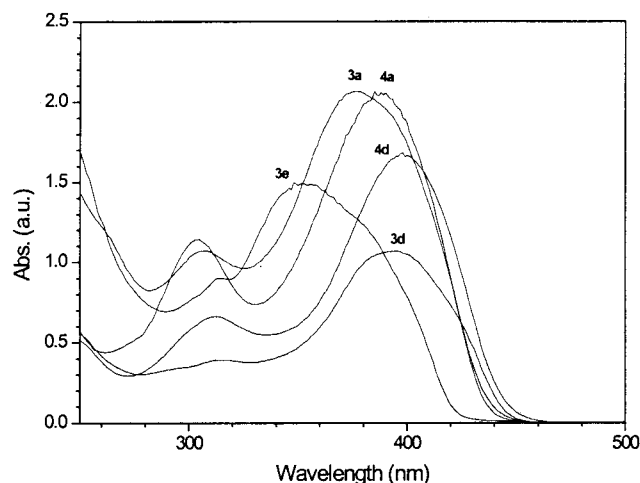


Figure 2. Electronic absorption spectra of **3a**, **3d**, **3e**, **4a**, and **4d** in dichloromethane solution.

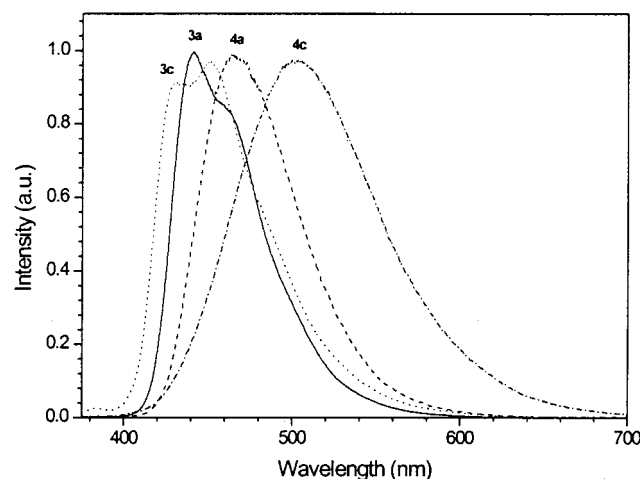


Figure 3. Emission spectra of **3a**, **3c**, **4a**, and **4c** in dichloromethane solution.

pared with those of the carbazole derivatives. The blue shift observed for **3b** and **4b** may be possibly due to the pronounced steric crowding in **4b**, which results in less coplanarity of the molecule.²⁵ Within a series, molecules with a longer conjugation spacer display red-shifted absorption (Figure 2). Thus, the fluorene-containing amines **3d** and **4d** possess the longest wavelength transitions. In comparison with that of **3a** (or **4a**), the steric hindrance of the meta-substituted diphenylamino units in **3b** (or **4b**) caused a blue shift of the absorption maxima. Additionally, the meta substitution could lead to less effective conjugation when compared to the para substitution.

All the compounds with the exception of **4c** and **4d** emit blue light when excited at 345 nm (Figure 3). Bright green emission was witnessed for **4c** and **4d**. Generally, the compounds reported here (**3a–e** and **4a–e**) possess moderately high fluorescence quantum yields (Φ_f). Compound **3a** possesses the highest quantum efficiency in the series. The improvement in quantum efficiency when compared to the 3,6-diamino-substituted carbazole derivatives we reported earlier¹⁴ may be attributed to the aryl spacers that separate the carba-

zole and diarylamine segments. This possibly minimizes the nonradiative electron-transfer reactions. It is very interesting to compare these molecules with type "A" (Figure 1) structural motifs. For instance, tris-1,3,5-(5-diphenylamino-2-thienyl)benzene, which is stripped of the phenyl spacer when compared to **4a**, exhibits only a weak blue emission ($\Phi_f = 0.03$).²⁶ Relatively lower quantum yield, larger Stokes shifts, and a much broader emission spectrum observed for **3b** and **4b** points out that the equilibrium geometry of these molecules are displaced at the excited states from its ground state.²⁷ In contrast, small Stokes shifts observed for the fluorene-incorporated compounds **3d** and **4d** are presumably due to the rigid bridged structure of fluorene that hinders the geometrical relaxation.

In general, the emission spectra of the carbazole derivatives **3a–3e** in solution display vibronic structures. However, in the condensed state, the vibronic structures in the emission were dramatically reduced for these derivatives. This means that the amorphism is enhanced in the solid state.²⁸ All the molecules except **4b** undergo a prominent red shift in their emission at the glassy state. Steric hindrance in **4b** possibly prohibits the intermolecular association and aggregation; thus, a blue shift is noticed. This observation points out that a sterically demanding structure is essential for retaining the solution emission color in the solid state.

Electrochemical Properties. Electrochemical characteristics of the star-shaped molecules were investigated by using cyclic and differential pulse voltammetric methods. The first oxidation potentials were used to determine the HOMO energy levels. Ferrocene served as an internal standard for calibrating the potential and calculating the HOMO levels (-4.8 eV).²⁹ The pertinent data are listed in Table 1.

In general, all the molecules undergo a reversible multielectron (two or three) oxidation arising from terminal diphenylamino units followed by a series of reversible or irreversible oxidations originating from bridging aromatic segments. The reversibility of the latter oxidations is largely governed by the spacers. Thus, the phenyl-, carbazole-, and fluorene-conjugated materials (**3a**, **3c**, **3d**, **4c**, and **4d**) display two or three reversible oxidations (Figure 4). The carbazole-cored derivatives (**3a** and **3d**) exhibit three reversible oxidations. The first two-electron oxidation is assigned to the simultaneous oxidation of the peripheral diphenylamino units while the next two one-electron oxidations stem from thiophene and carbazole cores. A reversible thiophene-based redox couple is located ca. +400 mV vs Fc/Fc⁺ when it is placed between two efficient donors.³⁰ Similarly, **4d** also undergoes three reversible oxidations. The first three-electron oxidation is located at the diphenylamino moieties and the next two consecutive one-electron processes originate from the cen-

(26) Lin, J. T., unpublished results.

(27) Yam, V. W. W.; Cheng, E. C. C.; Zhu, N. Y. *Angew. Chem., Int. Ed.* **2001**, *40*, 1763.

(28) Liu, B.; Yu, W.-L.; Lai, Y.-H.; Huang, W. *Chem. Mater.* **2001**, *13*, 1984.

(29) (a) Thelakkat, M.; Schmidt, H. *Adv. Mater.* **1998**, *10*, 219. (b) Hohle, C.; Hofmann, U.; Schloter, S.; Thelakkat, M.; Strohrriegel, P.; Haarer, D.; Zilker, S. *J. Mater. Chem.* **1999**, *9*, 2205.

(30) (a) Justin Thomas, K. R.; Lin, J. T.; Wen, Y. S. *Organometallics* **2000**, *19*, 1008. (b) Zhu, Y. B.; Wolf, M. O. *J. Am. Chem. Soc.* **2000**, *122*, 10121.

(25) Zhang, X. H.; Chen, B. J.; Lin, X. Q.; Wong, O. Y.; Lee, C. S.; Kwong, H. L.; Lee, S. T.; Wu, S. K. *Chem. Mater.* **2001**, *13*, 1565.

Table 2. Electroluminescence Data for the Compounds

	3a^a TPBI/Alq ₃	3b^a TPBI/Alq ₃	3c^a TPBI/Alq ₃	3e^a TPBI/Alq ₃	4a^a TPBI/Alq ₃	4b^a TPBI/Alq ₃	4c^a TPBI/Alq ₃	4e^b TPBI/Alq ₃
turn-on voltage, V	2.7/3.0	3.0/2.0	2.5/2.5	3.0/3.0	3.0/3.0	3.0/3.0	3.0/3.0	2.5/2.5
max brightness, Cd/m ²	19944/21330	10502/40215	20760/18500	20763/17270	16420/17001	3760/17850	2360/10440	11090/23150
max external quantum effic, %	1.67/0.76	1.78/1.50	1.30/0.66	1.30/0.66	1.32/0.86	0.59/0.88	0.59/0.88	0.65/0.99
max power effic, lm/W	1.41/1.70	2.00/3.07	2.05/1.31	1.25/0.96	1.35/1.23	0.37/1.25	0.15/0.46	0.79/1.55
λ _{em}	474/522	458/522	485/522	470/522	478/512	458/520	502/508	482/524
CIE, x,y	0.17, 0.20/0.31, 0.53	0.14, 0.14/0.31, 0.56	0.17, 0.25/0.31/0.53	0.17, 0.25/0.27, 0.53	0.18, 0.23/0.27, 0.46	0.16, 0.15/0.31, 0.47	0.27, 0.40/0.26, 0.47	0.19, 0.29/0.31, 0.50
voltage, ^c V	6.7/7.3	6.0/6.9	6.5/6.8	5.6/6.6	6.0/6.8	7.2/5.7	7.6/8.2	6.0/6.4
brightness, ^c Cd/m ²	2375/2305	2121/4395	1521/1544	2231/2026	1957/2017	664/2018	324/1103	1211/2604
external quantum effic ^c %	1.67/0.75	1.73/1.47	0.70/0.56	1.28/0.66	1.29/0.85	0.56/0.84	0.15/0.45	0.65/0.97
power effic, ^c lm/W	1.10/0.99	1.10/2.25	0.73/0.71	1.25/0.96	1.02/0.94	0.29/1.10	0.13/0.42	0.63/1.28

^a ITO/**3x** or **4x** (400 Å)/TPBI (400 Å)/Mg:Ag. ^b ITO/**3x** or **4x** (400 Å)/Alq₃ (400 Å)/Mg:Ag where **x** = **a**, **b**, **c**, or **e**. ^c Taken at a current density of 100 mA/cm².

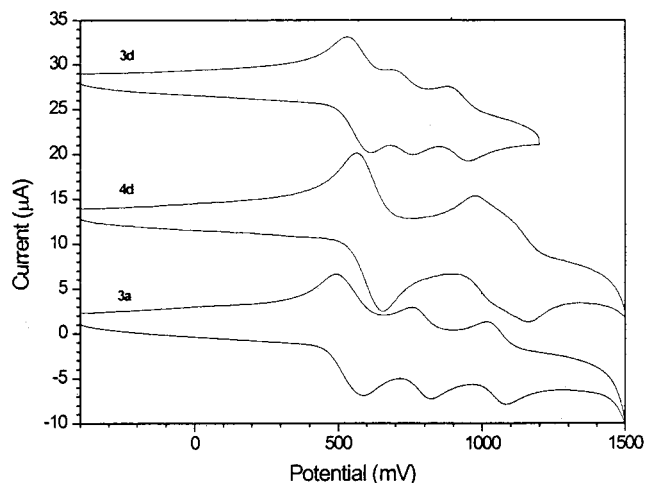


Figure 4. Cyclic voltammograms of the compounds **3a**, **3d**, and **4d**.

tral tris(thienyl)benzene core. Alternatively the carbazole-bridged analogues **3c** and **4c** exhibit two reversible oxidations originating from diphenylamino and carbazole/thiophene segments. One irreversible oxidation wave was observed for **3b**, **3e**, **4b**, and **4e** at potentials 0.728, 0.387, 0.780, and 0.536 V, respectively. They probably originate from the thiophene oxidation.

Upon comparison of the first oxidation potentials of the two classes of compounds, the following trends emerge: (a) The oxidations due to the diphenylamino unit appears at more positive potentials for the benzene-cored derivatives (**4a–4d**) than the carbazole-cored compounds (**3a–3d**). This could be possibly a result of a relatively strong electron-donating ability of carbazole core as compared with the benzene core. (b) The carbazole-armed materials (**3c**, **3e**, **4c**, and **4e**) similarly possess lowest first oxidation potentials within a series for the above-mentioned reason. (c) In general, for benzene-cored compounds the first oxidation shifts cathodically in the following order: **4b** > **4a** > **4d** > **4e** > **4c**. This order reflects the electron richness of the

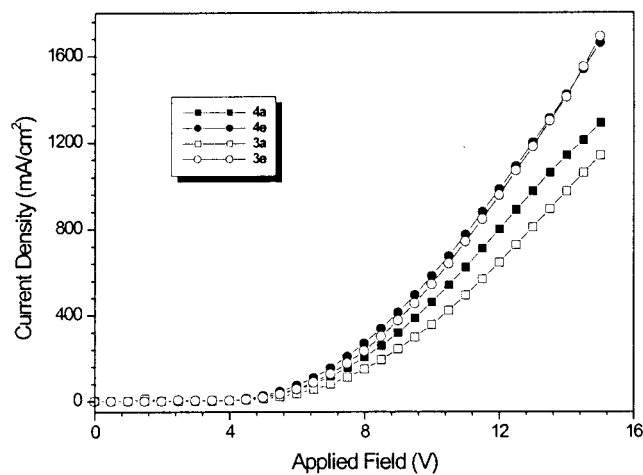
conjugation segment involved. Thus, the strongly electron-donating carbazole stabilizes the diphenylamino radical cation that results from anodic oxidation. This order is perturbed slightly in carbazole-based derivatives, **3b** > **3d** > **3a** > **3c** ≈ **3e**, due to the additional charge donation from carbazole core that will be effectively transmitted to the peripheral diphenylamine segment if the bridge is short.

Characteristics of Light-Emitting Devices. Except for **3d** and **4d**, which decomposed during vacuum deposition,³¹ all the compounds in this study were subjected to device fabrication. Two types of double-layer EL devices using **3** or **4** as a hole-transport layer and Alq₃ or TPBI as an electron-transporting layer were fabricated: (I) ITO/**3** (or **4**)/TPBI/Mg:Ag; (II) ITO/**3** (or **4**)/Alq₃/Mg:Ag. The salient parameters are compiled in Table 2 and the voltage, current density, luminance characteristics, and EL spectra are displayed in Figures 5–7 for selected materials. Green light characteristic of Alq₃ was emitted from type II devices, whereas type I devices emitted blue to green light from the compounds **3** or **4** in view of the close resemblance between EL and film PL spectra. Such an outcome can be rationalized by the HOMO energy gaps between the hole-transport and electron-transport materials. Passage of holes from **3** or **4** to TPBI is effectively blocked due to the low HOMO energy level of TPBI.³²

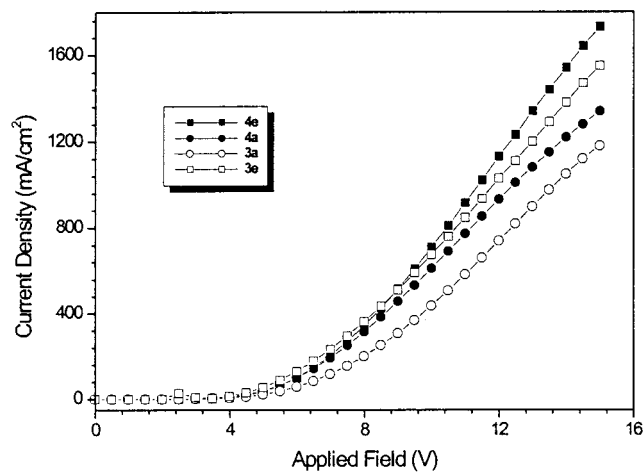
All the devices in this study exhibit relatively low turn-on voltages (2.5–3.0 V) and operating voltages (5.6–7.2 V at a current density of 100 mA/cm²). For type I devices, compounds **3x** (**x** = **a–e**) have better performance (external quantum efficiencies and luminous

(31) The deposition temperature is generally set at ≈330 °C. However, sublimation of compounds **3d** and **4d** need a higher temperature because of their low volatility. The evaporated films were analyzed differently from the original samples and remained uncharacterized.

(32) (a) Zhang, X. H.; Lai, W. Y.; Gao, Z. Q.; Wong, T. C.; Lee, C. S.; Kwong, H. L.; Lee, S. T.; Wu, S. K. *Chem. Phys. Lett.* **2000**, *320*, 77. (b) Tao, Y.-T.; Balasubramaniam, E.; Danel, A.; Jarosz, B.; Tomasik, P. *Appl. Phys. Lett.* **2000**, *77*, 933.



(a)

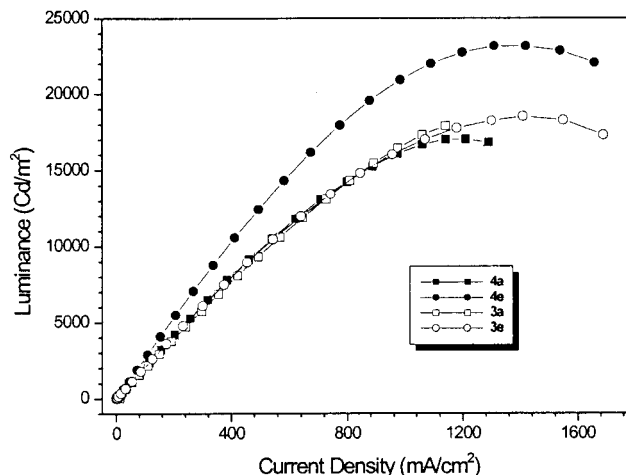


(b)

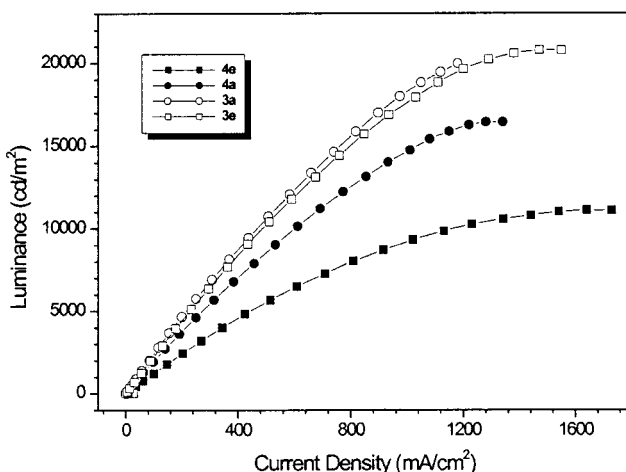
Figure 5. Applied field vs current density characteristics of compounds **3a**, **3e**, **4a**, and **4e** for (a) Alq₃ and (b) TPBI devices.

efficiencies at a current density of 100 mA/cm²) than **4x**. However, no obvious correlation of these data with the HOMO or LUMO energy gaps between **3** (or **4**) and TPBI or with the solution quantum efficiencies of the compounds could be established. The difference in hole-transport ability may be also important. In the device I of **4c**, a red emission at ≈ 640 nm was found to be mixed with the green light of **4c**. The origin of this red-shifted emission may be due to the exciplex formation³³ at the interface of **4c** and TPBI layers. Such an exciplex formation may partially account for the much inferior performance of the **4c** device than others. Although the lower energy gap between the HOMO of the hole-transport material (**4c**) and the LUMO of the electron-transport material (TPBI) facilitates the exciplex formation,¹² it is not obvious to us that **3c**, having a similar HOMO level to that of **4c**, did not form exciplex with TPBI. We believe that the sterically demanding spacers in the compounds synthesized here helps to suppress the exciplex formation.

It is interesting to note that the type I devices of **3a**, **3b**, **4a**, and **4b** emit blue light based on their Commis-



(a)



(b)

Figure 6. Current density vs luminance characteristics of compounds **3b** and **4b** for (a) Alq₃ and (b) TPBI devices.

sion Internationale d'Eclairage (CIE) chromaticity coordinates ((*x*, *y*): **3a**, (0.17, 0.20); **3b**, (0.14, 0.14); **4a**, (0.18, 0.23); **4b**, (0.16, 0.15)). The performance for **3a**, **3b**, and **4a** devices (brightness, external quantum efficiencies, and luminous efficiencies at a current density of 100 mA/cm²) appears to be promising (**3a**: 2375 Cd/m², 1.67%, 1.10 lm/W; **3b**: 2121 Cd/m², 1.73%, 1.10 lm/W; **4a**: 1957 Cd/m², 1.29%, 1.02 lm/W) when compared to the blue-emitting devices reported recently.^{31b,34}

Conclusions

Triaryl amines incorporating photoactive chromophores have been synthesized as building blocks for assembling carbazole- and benzene-based starlike molecules capable of hole transporting and light emitting in double-layer

(33) (a) Tamoto, N.; Adachi, C.; Nagai, K. *Chem. Mater.* **1997**, *9*, 1077. (b) Itano, K.; Ogawa, H.; Shirota, Y. *Appl. Phys. Lett.* **1998**, *72*, 636.

(34) (a) Hosokawa, C.; Higashi, H.; Nakamura, H.; Kusumoto, T. *Appl. Phys. Lett.* **1995**, *67*, 3853. (b) Gao, Z.; Lee, C. S.; Bello, I.; Lee, S. T.; Chen, R.-M.; Luh, T.-Y.; Shi, J.; Wang, C. W. *Appl. Phys. Lett.* **1999**, *74*, 865. (c) Balasubramaniam, E.; Tao, Y.-T.; Danel, A.; Tomasik, P. *Chem. Mater.* **2000**, *12*, 2788. (d) Leung, L. M.; Lo, W. Y.; So, S. K.; Lee, K. M.; Choi, W. K. *J. Am. Chem. Soc.* **2000**, *122*, 5640. (e) Tao, Y.-T.; Balasubramaniam, E.; Danel, A.; Jarosz, B.; Tomasik, P. *Chem. Mater.* **2001**, *13*, 1207. (f) Ko, C.-W.; Tao, Y.-T.; Danel, A.; Kremlínska, L.; Tomasik, P. *Chem. Mater.* **2001**, *13*, 2441.

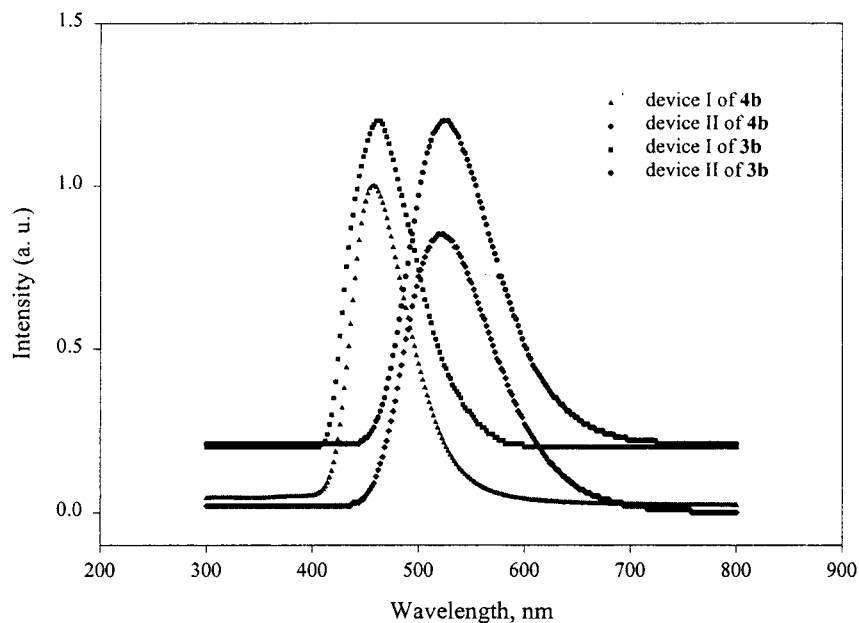


Figure 7. Comparison of the EL spectra of the compounds **4b** and **3b** in the two types of devices.

organic light-emitting diodes. The iterative procedures developed here could be further expanded to obtain dendrimers or high molecular weight polymers. Some compounds described in this report exhibit promising blue emission and OLED characteristics. Except for **4c**, no exciplex formation was found in devices fabricated. Evaluation of the morphology of these new compounds, effect of thickness on the performance of the devices, and lifetime of the devices will be studied soon. Efforts are also underway to synthesize molecules possessing unsymmetrical structures and dual functions (i.e., hole-

and electron-transporting segments) using the same strategy.

Acknowledgment. This work was supported by the Academia Sinica and National Science Council.

Supporting Information Available: Data are presented for compounds 2-(3,5-dibromophenyl)thiophene, **1b–e**, **2b–e**, **3b–e**, and **4b–e** (PDF). This material is available free of charge via the Internet at <http://pubs.acs.org>.

CM010976Q